The Hippocampus Rapidly Integrates Sequence Representations During Novel Multistep Predictions

Hannah Tarder-Stoll[1], Christopher Baldassano[2*], Mariam Aly[3*]

[1]Department of Psychology, Glendon Campus, York University, Toronto, ON, M4N 3M6
[2]Department of Psychology, Columbia University; New York, NY, 10027
[3]Department of Psychology, University of California, Berkeley; Berkeley, CA, 94720

*These authors contributed equally to this work

Abbreviated title: Hippocampal sequence integration supports prediction

Please address correspondence to:
Hannah Tarder-Stoll (htstoll@yorku.ca)

ORCiD:
Hannah Tarder-Stoll: https://orcid.org/0009-0007-0957-4499
Christopher Baldassano: https://orcid.org/0000-0003-3540-5019
Mariam Aly: https://orcid.org/0000-0003-4033-6134

Number of pages: 41

Number of figures: 5

Word count: Abstract – 184 words; Introduction – 782 words; Discussion – 1262 words

Conflict of Interest: The authors declare no competing financial interests.

Acknowledgements: This work was funded by a National Institutes of Health Research Project Grant (R01EY034436) and a Zuckerman Institute Seed Grant for MR Studies (CU-ZI-MR-S-0016) to M.A. and C.B. We would like to thank the Alyssano Group for helpful advice on this project.

Abstract

Memories for temporally extended sequences can be used adaptively to predict future events on multiple timescales, a function that relies on the hippocampus. For such predictions to be useful, they should be updated when environments change. We investigated how and when new learning shapes hippocampal representations of temporally extended sequences, and how this updating relates to flexible predictions about future events. Human participants learned sequences of environments in immersive virtual reality. They then learned novel environment transitions connecting previously separate sequences. During subsequent fMRI, participants predicted multiple steps into the future in both the newly connected sequence and control sequences that remained separate. The hippocampus integrated representations of the connected sequence, such that activity patterns became more similar across trials for the connected sequence vs. the unconnected sequences. These integrated sequence representations in the hippocampus emerged soon after learning, incorporated representations of the initial sequences as well as new activity patterns not previously present in either sequence, and predicted participants' ability to update their predictions in behavior. Together, these results advance our understanding of how structured knowledge dynamically emerges in service of adaptive behavior.

Introduction

Memories guide adaptive behavior by supporting predictions. Through repeated experience, the brain – particularly the hippocampus and surrounding medial temporal lobe cortex – creates predictive models that capture the temporal structure of the environment and support future-oriented behaviors at multiple timescales [1–3]. A common challenge, however, is that the environment's structure does not always remain stable. New information should cause us to update internal models of the environment to support flexible predictions about novel scenarios. For example, learning routes through a city allows us to plan trajectories multiple steps ahead. Upon learning that two seemingly separate routes are linked via a side street, we can plan trajectories along the connected route, even without direct experience [4–8]. Here, we investigated *when* and *how* new learning that connects previously separate, temporally extended sequences shapes hippocampal representations to support flexible prediction of novel trajectories.

The hippocampus is well situated to support flexible prediction because it represents temporal structure and integrates information learned across discrete episodes. For example, hippocampal sequence representations allow individuals to generate multistep predictions about future states [1,3,9,10]. Learning sequential structure requires forming connections among events, and indeed, the hippocampus supports integration across related experiences by linking episodes that share overlapping elements, even if these elements were not encountered close to one another in time [11–16]. In this way, flexible hippocampal representations build structured knowledge that generalizes beyond specific episodes, enabling inferences about novel relationships [16–18]. Yet, prior work has largely examined integration of simple, pairwise associations [11,12,19–27], and real-world environments often involve temporally extended event sequences. In these contexts, new information that links two previously unrelated sequences can

have broader consequences, potentially reshaping neural representations of the entire sequential structure even if the change occurs at a relatively local point. Open questions therefore remain about when integrative representations of sequences emerge, what information they contain, and how they influence prediction updating. Here, we investigated both the *time course* and *nature* of hippocampal representations that allow integration to update internal models of temporally extended experiences to guide future-oriented behavior.

We first focus on the time course of updating. In behavior, even brief learning episodes trigger rapid reconfiguration of structured knowledge [28,29]. However, it remains unclear whether new learning coincides with rapid updating of hippocampal representations, or whether these representations are reshaped gradually over time. The hippocampus is well-positioned to support rapid flexibility: it quickly encodes new associations [30,31] which may allow rapid incorporation of new information during planning [32]. However, updating knowledge of extended temporal structure can be supported by replay and consolidation [33–36]; thus, updated representations may take time to emerge. For instance, during rest, the hippocampus reactivates sequences that were never directly experienced [33,34], and this reactivation may reorganize internal models in service of future behavior [37–39]. Fast and slow updating are not mutually exclusive: rapid initial updating may be followed by slower changes.

After assessing the time course of hippocampal updating, we asked *how* the hippocampus may integrate memories for initially separate, temporally extended sequences when these sequences become connected by a new link. We investigated two questions about how connected sequence representations were related to their pre-integration representations (as opposed to being newly-generated patterns not present pre-integration; [13]). First, we tested whether a newly integrated sequence representation preserved at least some features of the individual, original sequences, exhibiting relative *stability* even after updating. Second, we tested

whether linking two sequences caused *blending* of their representations, such that the representation of one sequence inherited some of the original features of the other [1]. Stability and blending are not mutually exclusive: integration may result in representations that preserve elements of the original sequences, while also blending representations together or incorporating novel features.

To determine *when* and *how* hippocampal representations are updated after previously distinct sequences are connected, we asked participants to use sequence memories to anticipate events at multiple timescales (**Figure 1a**). After learning 4 sequences of virtual reality environments, participants learned novel, local event transitions that linked 2 of the previously separate sequences into a single, connected sequence (**Figure 1b**). The other 2 sequences remained separate and served as our baseline unconnected sequences. During fMRI, participants anticipated upcoming environments along both the connected and unconnected sequence conditions (**Figure 1c**). Critically, trials in the connected sequence required participants to traverse novel transitions. We examined patterns of activity in the hippocampus to: (1) determine whether trials in the connected vs. unconnected sequences were represented more similarly, indicating integration; (2) establish the temporal dynamics by which integration occurred; (3) test if hippocampal integration supported prediction along the connected sequence; and (4) characterize whether updated hippocampal representations retained stability with prior structure or blended features of connected sequences.

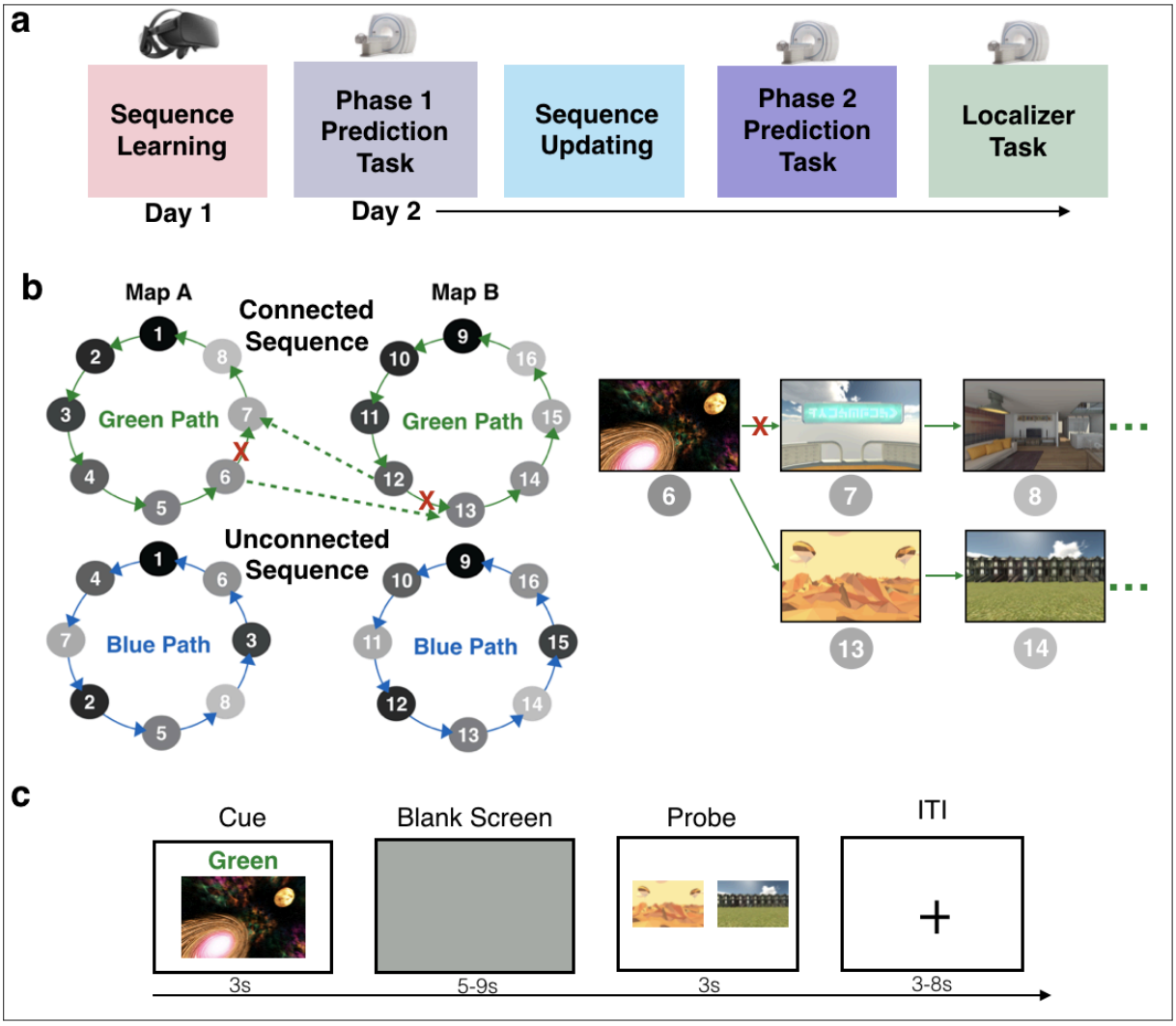

Figure 1 | **Sequence Structure and Prediction Task**. **(a)** Experiment overview. Day 1 sequence learning took place during immersive virtual reality. Day 2 tasks took place during fMRI. **(b)** Sequence structure. Stimuli were 8 environments in Map A and a different 8 in Map B (gray nodes). Participants learned 4 sequences, 2 in each map. Each map had one green path and one blue path (solid lines), traversing the same 8 environments in a different order. Participants predicted upcoming environments across both maps and paths. They then learned that one environment in Map A was now connected to one in Map B (dashed lines), and vice versa, on either the green or blue path (counterbalanced). They were told the old connections between these "bridge" environments no longer worked (red X) and they could only use the new ones, forming a single, connected map for one path. The other path remained unchanged. To learn the new connection, participants viewed an environment from Map A (on either path) and were told it now connected to an environment in Map B, and vice versa. **(c)** Participants made anticipatory judgments. They were cued with an image from either the connected or unconnected sequence, along with a path cue (Green or Blue). A blank screen followed, during which they predicted upcoming environments in the sequence. They were then probed with 2 images of upcoming environments and had to choose which was coming up sooner in the cued sequence.

Methods

Dataset

We used data from Tarder-Stoll, Baldassano*, & Aly* [3]. 32 participants (21 female; age: 19-35 years, mean = 24.17, sd = 4.11; education: 13-29 years, mean = 16.85, sd = 3.76) learned sequences of environments in immersive virtual reality (VR) and then, during fMRI, anticipated upcoming environments (**Figure 1a**).

Task Overview

Sequence Learning and the Phase 1 Prediction Task are not of primary interest, but for completeness are briefly described here and described in full in Tarder-Stoll et al. [3]. In the Sequence Learning task, participants learned 2 sequences ("Green Path" and "Blue Path") within each of 2 maps (Map A and Map B) in immersive VR, for a total of 4 sequences (**Figure 1b**). Map A and Map B contained 8 distinct environments each. Within each map, the Green Path and Blue Path contained the same environments in a different order. Participants learned the order of the 4 sequences by generating stories and then experiencing the environment sequences in immersive virtual reality using an Oculus Rift. Participants were then given a recall test to ensure they had learned all 4 sequences.

Participants returned one day later and completed the Phase 1 Prediction Task during fMRI (2 runs, 32 trials per run). In each trial, participants viewed an environment cue from a given map (A or B) and a path cue (Green or Blue) for 3 seconds. They then saw a blank screen for 5 to 9 seconds, followed by 2 images of upcoming environments. Participants indicated which of the 2 environments was coming up sooner in the sequence on the cued path (Green or Blue), relative to the cue environment. The correct answer could be 1 to 4 steps in the future. Participants had 3

seconds to respond, but were told that they could use the blank screen to predict upcoming environments in the order of the cued map and path. This task is analyzed in Tarder-Stoll et al., [3]. Here, this Phase 1 Prediction Task is solely used to explore how sequence representations change before vs. after sequence updating (see *fMRI Analysis).*

Sequence Updating

Next, participants completed the Sequence Updating task. Participants were told that one environment in Map A was now connected to one environment in Map B on either the Green or Blue Path. One environment in Map B also connected back to Map A, creating a single connected sequence encompassing all environments in both maps (**Figure 1b)**. The path (Green or Blue) that was the connected sequence was counterbalanced across participants, with the other path remaining unconnected across maps and serving as the baseline condition. For example, if a participant learned that the Green Path now connected Map A and Map B, the two Blue Paths (in Map A and Map B) would serve as the unconnected paths.

For the connected sequence, the environment that linked Map A to Map B (a "bridge environment") was randomly selected for each participant, as was the connecting environment in Map B. Following this new connection, the sequence of environments continued through all environments in Map B (in their previously learned order), and then linked back to Map A at the environment that had originally followed Map A's bridge environment, forming a circle of all 16 environments (**Figure 1b**). To learn these new connections, participants viewed a video of the bridge environment in Map A transitioning to Map B on the connected sequence (Green or Blue). They then viewed a video of the bridge environment in Map B transitioning back to Map A. Participants were told to think about how the new connections could be incorporated into the

stories that they had generated to learn the original sequences. Participants were then asked to recall the novel connections linking Map A and Map B.

Phase 2 Prediction Task

Participants then completed the primary task of interest during fMRI – the Phase 2 Prediction Task using the updated sequences (**Figure 1c)**. Participants predicted upcoming environments on the connected and unconnected sequences (4 runs, 24 trials per run). Participants were cued with an environment from one map (A or B) along with a path cue (Green or Blue) for 3 seconds. Participants then viewed a blank screen for a variable duration (5 to 9 seconds). Then, participants were presented with 2 images of upcoming environments and judged which was coming up sooner in the cued sequence, relative to the cue image. Participants were given 3 seconds to respond. This relatively short response deadline was implemented to encourage participants to use the blank screen period to generate predictions along the cued path in preparation for the forced-choice decision. The correct answer could be 1 to 4 steps away from the cue image. The incorrect answer could be a maximum of 5 steps away. There was a uniformly sampled 3 to 8 second jittered inter-trial interval (ITI), during which participants viewed a fixation cross. At the end of each run, there was a 60 second rest period during which participants viewed a blank screen.

Critically, when cued with the connected sequence (Green or Blue Path, counterbalanced across participants), participants were told to use the new connections they just learned that linked Map A and Map B. Thus, participants could be cued with an environment from Map A and the correct answer could be in Map B (**Figure 1c**). On the unconnected sequences, Map A and Map B remained separate.

In each of the 4 runs (9 minutes each), participants were cued with every environment from Map A and Map B on the connected sequence (16 environments across both maps) and with half of the environments from Map A and B on the unconnected sequences (8 environments across both maps) for a total of 24 trials per run. In the probe phase, the correct answer was equally distributed across steps into the future (1 to 4). The incorrect answer was randomly selected with the constraints that it must be at least 1 step in the future from the correct answer but no more than 5 steps in the future from the cue. Within a run, participants completed trials from the connected sequence and unconnected sequence conditions, blocked by condition; block order was randomized across runs and participants. The order of the cues was randomized and intermixed across Map (A or B) within each block.

Localizer Task

Next, participants completed 4 runs of the Localizer Task (4 minutes each). This allowed us to select voxels that reliably discriminated between environments and obtain environment-specific template patterns of brain activity across those voxels (see *fMRI Analysis*). Participants viewed all environments in a randomized order. They were first shown an environment *without* a path cue (Green or Blue) for 1 second. The absence of the path cue allowed us to obtain a context-independent pattern of brain activity for each environment. Participants then saw a blank screen for 5 seconds, during which they were told to imagine themselves in the environment in immersive virtual reality, where the environments had been learned. Participants then saw 8 images of the environment, 45° apart, for 4 seconds, to mimic a panorama. Finally, participants were given 3 seconds to rate how vividly their imagination matched these images. There was a uniformly jittered ITI between 3 and 8 seconds.

Behavioral Analysis

Behavioral data were analyzed in R with t-tests and generalized linear and linear mixed effects models (GLMMs and LMMs, glmer and lmer function in the *lme4* package; [40]). For analyses that modeled multiple observations per participant, such as accuracy or response time on a given trial, models included random intercepts and slopes for all within-participant effects. All response time models examined responses on correct trials only.

We first ensured that participants performed effectively during the Phase 2 Prediction Task, across both conditions, by comparing accuracy to chance (50%) using a one-sample t-test. We then conducted two one-sample t-tests comparing performance on the Phase 2 Prediction Task to chance separately for the connected and unconnected sequence conditions.

Next, we examined how performance changed across runs on the Phase 2 Prediction Task. We used a GLMM to model trial-wise accuracy as a function of condition (unconnected sequences = -0.5, connected sequence = 0.5), run (run 1 = -0.75, run 2 = -0.25, run 3 = 0.25, run 4 = 0.75), and their interaction.

Within the connected sequence condition, there were 3 trial types: (1) trials in which both probes were in the same map as the cue (same-map trials; these do not require crossing the bridge environment); (2) trials in which one probe was in a different map than the cue (one-different trials; these trials also do not require crossing the bridge environment because the environment in the same map is always the correct answer); and (3) trials in which both probes were in a different map than the cue (different-map trials; these trials require crossing the bridge environment; **Figure 2**). We tested whether accuracy differed as a function of trial type

(same-map = 0, one-different = 1, different-map = 2), run (run 1 = -0.75, run 2 = -0.25, run 3 = 0.25, run 4 = 0.75), and their interaction. Trial type was a dummy-coded factor, allowing us to investigate how performance changed on one-different and different-map trials, relative to same-map baseline.

MRI Acquisition

MRI acquisition was reported in Tarder-Stoll et al. [3] and reiterated here for convenience. We collected whole-brain fMRI data using a 64-channel head coil on a 3 Tesla Siemens Magnetom Prisma scanner. We first acquired T1 structural scans using a magnetization-prepared rapid acquisition gradient-echo (MPRAGE) sequence. Functional images used a multiband echo-planar imaging (EPI) sequence (repetition time = 1.5s, echo time = 30ms, in-plane acceleration factor = 2, multiband acceleration factor = 3, voxel size = 2mm iso). There were 69 oblique axial slices collected in an interleaved order, with slices tilted -20 degrees relative to the AC-PC line. At the end of the session, we collected field maps (TR = 679 ms, TE = 4.92 ms/7.38 ms, flip angle = 60°, 69 slices, 2 mm isotropic).

Preprocessing

Results included in this manuscript come from preprocessing performed using *fMRIPrep* 1.5.2 (Esteban, Markiewicz, et al. (2018); Esteban, Blair, et al. (2018); RRID:SCR_016216), which is based on *Nipype* 1.3.1 (Gorgolewski et al. (2011); Gorgolewski et al. (2018); RRID:SCR_002502).

Anatomical data preprocessing

The T1-weighted (T1w) image was corrected for intensity non-uniformity (INU) with N4BiasFieldCorrection (Tustison et al. 2010), distributed with ANTs 2.2.0 (Avants et al. 2008, RRID:SCR_004757), and used as T1w-reference throughout the workflow. The T1w-reference was

then skull-stripped with a *Nipype* implementation of the antsBrainExtraction.sh workflow (from ANTs), using OASIS30ANTs as target template. Brain tissue segmentation of cerebrospinal fluid (CSF), white-matter (WM) and gray-matter (GM) was performed on the brain-extracted T1w using fast (FSL 5.0.9, RRID:SCR_002823, Zhang, Brady, and Smith 2001). Brain surfaces were reconstructed using recon-all (FreeSurfer 6.0.1, RRID:SCR_001847, Dale, Fischl, and Sereno 199981), and the brain mask estimated previously was refined with a custom variation of the method to reconcile ANTs-derived and FreeSurfer-derived segmentations of the cortical gray-matter of Mindboggle (RRID:SCR_002438, Klein et al. 2017). Volume-based spatial normalization to one standard space (MNI152NLin2009cAsym) was performed through nonlinear registration with antsRegistration (ANTs 2.2.0), using brain-extracted versions of both T1w reference and the T1w template. The following template was selected for spatial normalization: *ICBM 152 Nonlinear Asymmetrical template version 2009c* [Fonov et al. (2009)83, RRID:SCR_008796; TemplateFlow ID: MNI152NLin2009cAsym].

Functional data preprocessing

For each of the 10 BOLD runs found per subject (across all tasks and sessions), the following preprocessing was performed. First, a reference volume and its skull-stripped version were generated using a custom methodology of *fMRIPrep*. A deformation field to correct for susceptibility distortions was estimated based on a field map that was co-registered to the BOLD reference, using a custom workflow of *fMRIPrep* derived from D. Greve's epidewarp.fsl script and further improvements of HCP Pipelines (Glasser et al. 2013). Based on the estimated susceptibility distortion, an unwarped BOLD reference was calculated for a more accurate co-registration with the anatomical reference. The BOLD reference was then co-registered to the T1w reference using bbregister (FreeSurfer) which implements boundary-based registration (Greve and Fischl 2009). Co-registration was configured with six degrees of freedom. Head-motion parameters with

respect to the BOLD reference (transformation matrices, and six corresponding rotation and translation parameters) are estimated before any spatiotemporal filtering using mcflirt (FSL 5.0.9, Jenkinson et al. 2002). The BOLD time-series, were resampled to surfaces on the following spaces: *fsaverage6*. The BOLD time-series (including slice-timing correction when applied) were resampled onto their original, native space by applying a single, composite transform to correct for head-motion and susceptibility distortions. These resampled BOLD time-series will be referred to as *preprocessed BOLD in original space*, or just *preprocessed BOLD*. The BOLD time-series were resampled into standard space, generating a *preprocessed BOLD run in ['MNI152NLin2009cAsym'] space*. First, a reference volume and its skull-stripped version were generated using a custom methodology of *fMRIPrep*. Several confounding time-series were calculated based on the *preprocessed BOLD*: framewise displacement (FD), DVARS and three region-wise global signals. FD and DVARS are calculated for each functional run, both using their implementations in *Nipype* (following the definitions by Power et al. 2014). The three global signals are extracted within the CSF, the WM, and the whole-brain masks. Additionally, a set of physiological regressors were extracted to allow for component-based noise correction (*CompCor*, Behzadi et al. 2007). Principal components are estimated after high-pass filtering the *preprocessed BOLD* time-series (using a discrete cosine filter with 128s cut-off) for the two *CompCor* variants: temporal (tCompCor) and anatomical (aCompCor). tCompCor components are then calculated from the top 5% variable voxels within a mask covering the subcortical regions. This subcortical mask is obtained by heavily eroding the brain mask, which ensures it does not include cortical GM regions. For aCompCor, components are calculated within the intersection of the aforementioned mask and the union of CSF and WM masks calculated in T1w space, after their projection to the native space of each functional run (using the inverse BOLD-to-T1w transformation). Components are also calculated separately within the WM and CSF masks. For

each CompCor decomposition, the *k* components with the largest singular values are retained, such that the retained components' time series are sufficient to explain 50 percent of variance across the nuisance mask (CSF, WM, combined, or temporal). The remaining components are dropped from consideration. The head-motion estimates calculated in the correction step were also placed within the corresponding confounds file. The confound time series derived from head motion estimates and global signals were expanded with the inclusion of temporal derivatives and quadratic terms for each (Satterthwaite et al. 2013). Frames that exceeded a threshold of 0.5 mm FD or 1.5 standardised DVARS were annotated as motion outliers. All resamplings can be performed with *a single interpolation step* by composing all the pertinent transformations (i.e. head-motion transform matrices, susceptibility distortion correction when available, and co-registrations to anatomical and output spaces). Gridded (volumetric) resamplings were performed using antsApplyTransforms (ANTs), configured with Lanczos interpolation to minimize the smoothing effects of other kernels (Lanczos 1964). Non-gridded (surface) resamplings were performed using mri_vol2surf (FreeSurfer).

Many internal operations of *fMRIPrep* use *Nilearn* 0.5.2 (Abraham et al. 2014, RRID:SCR_001362), mostly within the functional processing workflow. For more details of the pipeline, see the section corresponding to workflows in *fMRIPrep*'s documentation (https://fmriprep.org/en/latest/workflows.html).

Copyright Waiver

The above boilerplate text was automatically generated by fMRIPrep with the express intention that users should copy and paste this text into their manuscripts *unchanged*. It is released under the CC0 license.

fMRI Analysis

Analyses were performed in Python and R. Representational similarity analyses [41] were performed using custom code in Python 3. Statistical analysis comparing pattern similarity across conditions, correlations between fMRI results and behavior, and visualizations were performed using custom code in R.

Conjunction ROI Definition

Our primary region of interest (ROI) was the hippocampus. We also conducted analyses in early visual cortex as a control ROI. We used a conjunction approach to identify voxels within these regions that reliably discriminated between environments (as in [3]). We defined an anatomical hippocampus ROI from the Harvard-Oxford probabilistic atlas in FSL (threshold: p = 0.50) and a visual cortex ROI (V1-V4) from the probabilistic human visual cortex atlas provided in Wang et al ([42]; threshold: p = 0.50). The ROIs and functional data were both transformed into 2 mm MNI space (MNI152NLin2009cAsym). We then identified voxels within these ROIs whose responses to the environments were consistent across participants using the same approach from Tarder-Stoll et al. [3], which was adapted from Tarhan and Konkle [43].

We first conducted a whole-brain GLM (in Python) predicting univariate activity from task and nuisance regressors during the Localizer Task. For each participant, we modeled BOLD activity for each of the 16 environments, collapsed across runs. The regressors for each environment included both viewing and imagination periods (see *Methods/Task Overview*). The model also included nuisance regressors: translation and rotation along the X, Y, and Z axes and their derivatives, motion outliers as determined by fMRIprep, CSF, white matter, framewise displacement, and discrete cosine-basis regressors for periods up to 125 seconds). We then

extracted the beta weights for each environment for each participant from the whole-brain GLM for each voxel in our atlas-based hippocampus and visual cortex ROIs. We then computed, for each voxel, the Pearson correlation between each participant's vector of beta weights (one beta weight for each environment) and the average vector of the remaining participants. An environment reliability score was calculated by averaging these correlations across all iterations of the held-out participant, and we only included voxels with an environment reliability score of 0.1 or greater in our final analyses. Thus, ROI selection was conducted using a set of data that was independent from the main analyses of the Prediction Task. We used these conjunction ROIs (156 voxels in hippocampus; 2931 voxels in visual cortex) for subsequent analyses.

Phase 2 Prediction Task Analysis

We used Python to run GLMs predicting whole-brain univariate BOLD activity from task and nuisance regressors from the Phase 2 Prediction Task. For each participant, we modeled BOLD activity separately for each run with regressors for the cue, blank screen, and probe periods, separately for each cued environment in Map A and Map B (1 to 16) and for each path (Green Path and Blue Path). This resulted in 32 task regressors for each phase (cue, blank screen, probe) of the Phase 2 Prediction Task per run. We also included nuisance regressors (translation and rotation along the X, Y, and Z axes and their derivatives, motion outliers as determined by fmriprep, CSF, white matter, framewise displacement, and discrete cosine-basis regressors for periods up to 125 seconds). The resulting beta weights for our task regressors for each run were examined within our hippocampal and visual cortex conjunction ROIs.

Pattern similarity analyses were conducted to examine how sequence representations in hippocampus and visual cortex changed across maps in the connected vs. unconnected sequence conditions. For each participant, we obtained the correlation between (1) the blank

screen pattern of activity on each trial and (2) the blank screen pattern of activity for all other trials in the same condition (connected sequence or unconnected sequences) but with a cue from the other map (A or B) (**Figure 3a**). For example, if the cue environment on a given trial was from Map A and in the connected sequence, we obtained the correlation between that trial's blank screen activity pattern and the blank screen activity patterns for trials in which the cue environment was in Map B and in the connected sequence. To explore how across-map pattern similarity changes across the Phase 2 Prediction Task while accounting for temporal autocorrelation within a run, we conducted this analysis across neighboring runs separately for early runs (1 & 2) and late runs (3 & 4). For example, if a trial was from run 1, we obtained the correlation with trials from the same condition and different map in run 2 and vice versa (**Figure 3a**).

The resulting correlations indicate the similarity between patterns of activity for Map A and Map B across runs. We tested for significant differences between the connected and unconnected sequence conditions with a paired-samples t-test. We ran follow-up paired-sample t-tests to assess differences in pattern similarity for early and late runs in the connected sequence, compared to averaged pattern similarity across all runs in the unconnected sequence condition. We opted to average across runs in the unconnected sequence condition because (1) we did not find differences in pattern similarity across runs for this condition and (2) we did not have enough trials to reliably estimate run-wise pattern similarity values in the unconnected sequences (8 trials per run, half the number of trials as the connected sequence; [44]).

To determine if pattern similarity was driven by changes in overall activity, we conducted univariate analyses by obtaining the average beta weight across all voxels in our hippocampus conjunction ROI, separately for the connected and unconnected sequence conditions. We

conducted these analyses across all runs, and separately for early and late runs. Further, we separately examined Cue and Blank Screen periods of the Phase 2 Prediction Task (**Figure 1c**). For each approach we compared univariate activity in the connected and unconnected sequence conditions using paired sample t-tests.

Relationship Between Prediction Task Pattern Similarity and Behavior

We determined whether across-map pattern similarity in hippocampus or visual cortex was related to performance (**Figure 4**). We performed an individual differences analysis in which we used the unconnected sequences condition as a baseline and examined whether changes in neural representations for the connected vs. unconnected sequences were related to behavioral differences across these conditions. We obtained the Spearman rank-order correlation between (1) the difference between participants' accuracy in the connected vs. unconnected sequence condition and (2) the difference between participants' hippocampal across-map pattern similarity in the connected vs. unconnected sequence condition.

Tests of Representational Stability and Blending

We conducted two analyses to investigate the nature of updated representations in the hippocampus for the connected sequences. One analysis examined if there was *stability* of representations for a given sequence from pre- to post-updating; the other analysis looked for *blending* of sequence representations after updating (**Figure 5**).

To investigate if there was *stability* of individual sequence representations in the newly connected sequence, we tested if trials from a given sequence after sequence updating were more similar to trials in the same sequence before updating than they were to trials in the same map for the unconnected sequence condition. Specifically, for each participant, we obtained the

correlation between the blank screen activity pattern during the Phase 2 Prediction Task for each connected sequence trial and two types of trials from the Phase 1 Prediction Task: (1) trials from the same map in the connected sequence, and (2) trials from the same map in the unconnected sequence. For example, if a Phase 2 Prediction Task trial came from Map A in the connected sequence, we calculated its similarity to Phase 1 Prediction Task trials from Map A in the connected sequence (same sequence) and from Map A in the unconnected sequence (same environments in a different order). We compared these pattern similarity values using a paired-samples t-test. This allowed us to assess whether Phase 2 representations in the connected sequence were more similar to their own Phase 1 representations than to the Phase 1 representations of the same map in the unconnected sequence condition. Critically, because Map A (and, separately, Map B) in the connected and unconnected sequence conditions have the same environments in a different order, this comparison allows us to control for pattern similarity driven only by repetition of the same environments.

We next tested whether updated representations in the connected sequence condition reflected a *blend* of Map A and Map B sequences. If so, post-updating representations of Maps A and B in the connected sequence may "inherit" features from the newly connected sequence's representations prior to learning. That is, Map A post-updating may contain features of Map B from pre-updating and vice versa. To test this, for each participant, for both the connected and unconnected sequences, we obtained the correlation between (1) the blank screen pattern of activity on each trial in the Phase 2 Prediction Task and (2) the blank screen pattern of activity for all trials with a cue from the other map (A or B) in the Phase 1 Prediction Task. For example, if the cue environment on a Phase 2 Prediction Task trial came from Map A, we obtained the correlation between its blank screen activity pattern and activity patterns from Phase 1 Prediction

Task trials with cue environments from Map B. This was done for the connected sequence and unconnected sequences separately, and those two values were then compared with a paired samples t-test. This allowed us to determine if representations carried over from Phase 1 to Phase 2 more strongly for the connected vs. unconnected sequences.

Results

Prediction Task Performance

In the Phase 2 Prediction Task, participants chose the probe that was coming up sooner relative to the cued environment 85.97% of the time, which was significantly above chance (50%, $t(31) = 51.057$, $p < 0.000001$). Performance was high and significantly above chance in both the unconnected sequence condition ($M_{accuracy} = 89.453\%$, $t(31) = 59.774$, $p < 0.000001$) and the connected sequence condition ($M_{accuracy} = 84.228\%$, $t(31) = 41.814$, $p < 0.000001$).

To determine how sequence memories are updated with experience, we tested how performance on the Phase 2 Prediction Task varied by condition and run. Performance was significantly higher in the unconnected vs. connected sequence condition (beta = -0.389, 95% CI = [-0.741, -0.037], p = 0.03; **Figure 2a**). Overall, performance did not significantly differ across runs of the Phase 2 Prediction Task (beta = 0.244, 95% CI = [-0.024, 0.513], p = 0.074; **Figure 2a**). However, there was a significant interaction between condition and run (beta = 0.742, 95% CI = [0.209, 1.276], p = 0.006; **Figure 2a**), such that performance increased across runs in the connected sequence condition (beta = 0.62, 95% CI = [0.329, 0.911], p = 0.00003), but not the unconnected sequence condition (beta = -0.122, 95% CI = [-0.563, 0.320], p = 0.588). In fact, performance in the connected sequence condition reached that of the unconnected sequence condition by the end of the task (beta = -0.150, 95% CI = [-0.874, 0.573], p = 0.684). Strikingly, even

in the first run of the Phase 2 Prediction Task, performance was high and significantly above chance in the connected sequence condition (average accuracy = 78.52%, $t(31) = 30.538$, $p < 0.000001$), suggesting that participants rapidly updated their memories to reflect the connected sequence structure.

We next examined how performance changed as a function of run and trial type in the connected sequence condition. Trials in this condition differed in difficulty based on whether participants needed to mentally traverse between maps to correctly anticipate upcoming environments (**Figure 2b**, see *Methods*). Trials in which both probes were in the same map as the cue (same-map trials) should be easier than trials in which the probes were in the different map from the cue (different-map trials), because different-map trials required participants to cross the bridge environment to correctly respond. Trials in which only one of the probes is in the different map from the cue (one-different trials) should be easier than both same-map and different-map trials, because a participant should be able to reject the incorrect probe on the basis of map identity alone, rather than temporal order. Specifically, because the correct answer was at most four steps away, it is never possible for the different-map environment to be closer than the same-map environment.

Indeed, accuracy in the connected sequence condition was highest on one-different trials (mean = 88.9%), followed by same-map trials (mean = 87.8%), and lowest on different-map trials (mean = 78.5%). There was a trend toward lower accuracy on different-map compared to same-map trials (beta = -0.368, 95% CI = [-0.744, 0.007], $p = 0.054$; **Figure 2b**), but there was no difference between one-different and same-map trials (beta = 0.284, 95% CI = [-0.139, 0.708], $p = 0.188$). Critically, there was a trial type by run interaction (beta = 0.585, 95% CI = [0.078, 1.091], $p = 0.024$;

Figure 2b), such that performance on different-map trials increased across runs more than performance on the baseline same-map trials. In the first run of the Phase 2 Prediction Task, accuracy was significantly lower on different-map trials compared to same-map trials (beta = -0.8726, 95% CI = [-1.361, -0.384], p = 0.0005), but performance on different-map trials reached that of same-map trials in the final run (beta = -0.086, 95% CI = [-0.701, 0.529], p = 0.784). Importantly, performance on different-map trials was above chance even in the first run (t(31) = 3.340, p = 0.002), again showing successful rapid updating of predictions in the connected sequence. In contrast, there was no interaction between same-map and one-different trials across runs (beta = -0.002, 95% CI = [-0.650, 0.645], p = 0.994). Together, these analyses show that trials in which participants had to mentally traverse the bridge environments linking Map A and B (i.e., different-map trials) improved the most over the course of the Phase 2 Prediction Task.

Thus, participants updated their memories of temporal structure after a single learning episode to successfully make predictions. Sequence memories reflected the new sequence structure even in the first run of the Phase 2 Prediction Task, but behavior continued to improve – implying both rapid and gradual updating of learned representations.

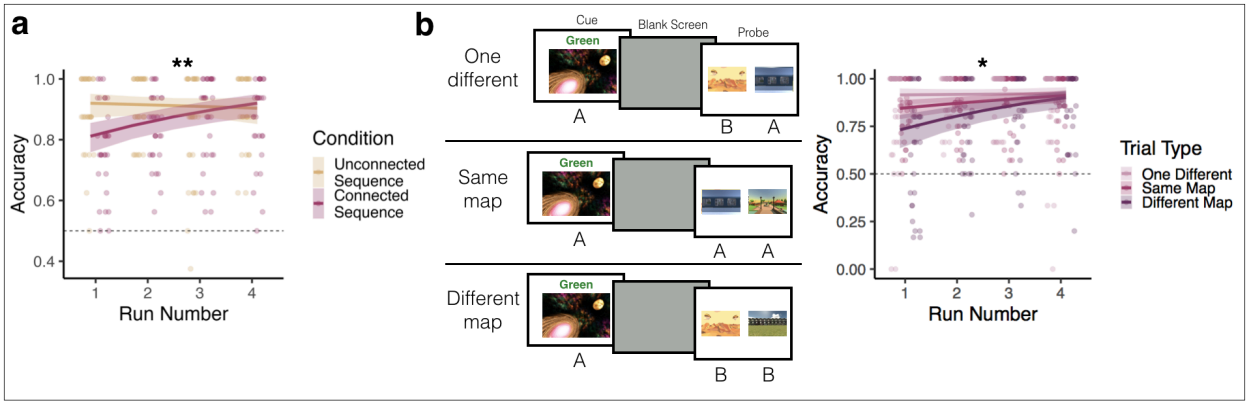

Figure 2 | Prediction Task Performance. (a) Overall Behavioral Performance. Solid lines and error ribbons indicate model predictions with 95% confidence intervals; points indicate individual participants' performance for each run. ** $p < .001$ for condition by run interaction. **(b)** Performance by trial type in the connected sequence condition. See main text for description of trial types. Performance was highest on one-different, followed by same-map, and then different-map trials. Performance improved the most across runs on different-map trials. Solid lines and error ribbons indicate model predictions with 95% confidence intervals; points indicate individual participants' performance for each run. * $p < 0.05$ for trial type by run interaction.

Integration of Hippocampal Sequence Representations

We next explored how updated sequences are represented in the hippocampus. We used multivoxel pattern analysis to determine if the connected sequence was represented more similarly than the unconnected sequences, consistent with hippocampal integration mechanisms [12]. We obtained the correlation between multivoxel patterns of activity elicited during the blank screen of the Phase 2 Prediction Task for trials in which cue environments came from Map A vs. Map B, separately for the connected and unconnected sequence conditions (see *Methods*; **Figure 3a**). Across-map pattern similarity was higher in the connected vs. unconnected sequence condition ($t(31) = 2.070$, $p = 0.041$; **Figure 3b**), indicating that hippocampal representations of Map A and Map B sequences were more similar when they were connected by the bridge environments. This confirms that the hippocampus supports updating of sequence memories by forming an integrated representation of the previously separate sequences. In contrast, across-map pattern similarity in visual cortex did not differ between the connected vs. unconnected sequence conditions ($t(31) = -0.279$, $p = 0.781$).

To probe how hippocampal sequence representations are updated over time, we separately compared across-map pattern similarity in the connected sequence for early and late runs to the averaged across-map pattern similarity in the unconnected sequences. In early runs, hippocampal across-map pattern similarity was significantly higher in the connected vs. unconnected sequence condition ($t(31) = 2.665$, $p = 0.012$; **Figure 3b**). In late runs, across-map

pattern similarity was not different in the connected vs. unconnected sequence conditions (t(31) = 1.304, p = 0.203; **Figure 3b**). There was a trending difference between early vs. late run across-map pattern similarity in the connected sequence condition (t(31) = -1.78, p = 0.085). We address this pattern in the Discussion. We then did the same early vs. late run analysis in visual cortex, and there was no difference in across-map pattern similarity between conditions, neither in early runs (t(31) = 0.244, p = 0.808) nor late runs (t(31) = 0.342, p = 0.734). Together, these results show that the hippocampus, but not visual cortex, integrates sequence representations in light of new information, and that this integration in hippocampus appears rapidly – in the first runs after new learning.

Integration of associated stimuli is linked to overall activity in the hippocampus [45]. We therefore investigated whether representational differences between conditions were due to differences in hippocampal univariate activity. Unlike across-map pattern similarity, there were no differences in hippocampal univariate activity between the connected and unconnected sequence conditions, either during the cue (t(31) = -1.404, p = 0.170) or the blank screen (t(31) = -0.081, p = 0.936) portion of the Phase 2 Prediction Task. There was no significant difference between conditions during early runs (cue: t(31) = -1.105, p = 0.278; blank screen: t(31) = -0.710, p = 0.483) or during late runs (cue = t(31) = -0.871, p = 0.390; blank screen: t(31) = 0.476, p = 0.638). Thus, the increase in across-map pattern similarity in the connected vs. unconnected sequence condition cannot be attributed to overall changes in hippocampal univariate activity.

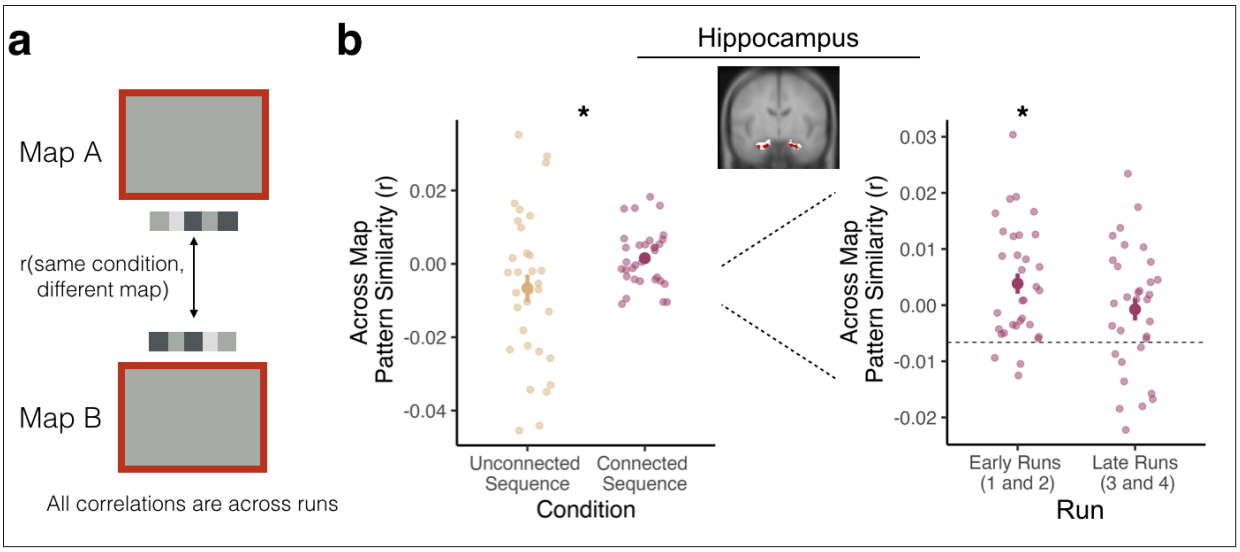

Figure 3 | **Sequence Integration in Hippocampus. (a)** Pattern similarity analysis. To quantify across-map pattern similarity during the Phase 2 Prediction Task, we obtained the correlation between (1) the blank screen pattern of activity on each trial and (2) the blank screen pattern of activity for all other trials in the same condition (connected sequence or unconnected sequences) but from the different map (A or B) for each participant. **(b)** Pattern similarity results. Left: We investigated across-map pattern similarity within our hippocampus conjunction ROI, collapsed across early and late runs. Across-map pattern similarity was higher for the connected sequence compared to the unconnected sequences. Note that the higher variance in the unconnected sequence condition is likely due to fewer trials in this condition. Right: Across-map pattern similarity was higher in early runs of the connected sequence condition compared to the unconnected sequence condition. There was no significant difference between conditions in late runs. Large points indicate the group average across-map pattern similarity, error bars indicate standard error of the mean, and small, transparent points indicate each participant's across-map pattern similarity. Dashed line indicates group average value in the unconnected sequence. * $p < .05$

Rapid Sequence Integration Supports Memory Updating

We next explored whether rapid sequence updating in the hippocampus was related to behavior. Overall, participants tended to show behavioral costs for the connected vs. unconnected sequence condition, at least in early runs (**Figure 2a**). We asked whether participants who showed more evidence for hippocampal integration for the connected sequence, compared to the baseline unconnected sequences, exhibited reduced behavioral costs (or behavioral benefits) for the connected vs. unconnected sequences. We obtained the Spearman's rank-order correlation between (1) the difference in hippocampal across-map similarity in the connected vs.

unconnected sequence conditions and (2) the behavioral difference between the connected vs. unconnected sequence conditions (see *Methods*). As a control analysis, we also calculated the Spearman's rank-order correlation with across-map pattern similarity in visual cortex. We found a positive relationship in the hippocampus (Spearman's *rho* = 0.368, p = 0.038; **Figure 4a**): participants who showed the most across-map integration for the connected (vs. unconnected) sequence exhibited reduced behavioral costs (or even behavioral benefits) in the connected (vs. unconnected) sequence condition. The same analysis in visual cortex was not statistically significant (Spearman's *rho* = 0.055, p = 0.763). Thus, increased across-map pattern similarity in hippocampus, but not visual cortex, was associated with reduced costs to prediction performance after sequence updating.

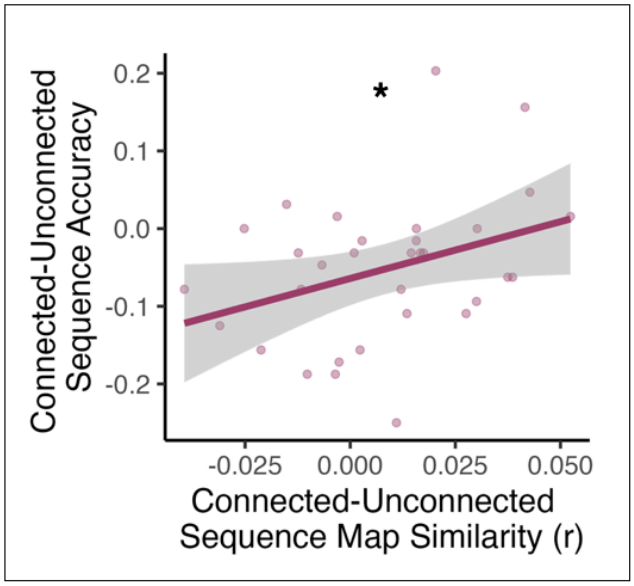

Figure 4 | Across-map pattern similarity in the hippocampus supports behavioral predictions. Greater across-map pattern similarity in the hippocampus for connected vs. unconnected sequences was associated with reduced behavioral costs for the connected sequence during the Prediction Task. Pink line and gray error ribbons indicate the correlation with 95% confidence intervals; points indicate each participant's across-map pattern similarity and Prediction Task performance. * p < .05

What is the nature of the post-updating, integrated representations in the hippocampus? Previously separate sequences become more similar after new learning (**Figure 3**), which could be due to the creation of a new (shared) representation, whose features were not present in either sequence prior to integration [13]. It is also possible that some features of the pre-integration representations persist even after sequence updating. For example, the two connected sequences may maintain some *stability* with their individual pre-updating representations. An alternative possibility (but not mutually exclusive), is that across-map integration results in a mixture of the two original sequences — with *blended* representations of Map A and Map B in the connected, but not the unconnected, sequence.

To look for stability in representations, we tested whether each component of the connected sequence (Map A and Map B environments in the connected path) showed similarity with their *pre-updating* representations (**Figure 5**). We compared these values to a baseline that controlled for pattern similarity driven by repetition of the same visual images, by obtaining the correlation between the Phase 2 representations of each Map in the connected sequence and the Phase 1 representations of the same Map in the unconnected sequence condition, which had the same environments in a different order. For example, the stability of the connected sequence in Map A was assessed by determining if its Phase 2 representation was more similar to its Phase 1 representation than to the Phase 1 representation of the unconnected sequence in Map A. Thus, this analysis allowed us to examine whether sequences that became connected retained similarity to their original representations, above and beyond any generic pattern similarity driven by repetition of the same images. To look for evidence of blended representations in the connected sequences, we tested whether Map A after updating became more similar to Map B

before updating (and vice versa) in the connected sequence condition compared to the same comparisons for the unconnected sequence condition. This would suggest that after sequences became connected, Map A inherited features of Map B, and vice versa – beyond the level of blending present for the unconnected sequences.

We found evidence for stability in hippocampal representations for the connected sequences, such that their post-updating representations retained features of their pre-updating representations ($t(31) = 2.15$, $p = 0.039$). Thus, the hippocampus can rapidly update representations of sequences in a way that partially maintains their prior identities but also links them together. We found no evidence for blended representations of the two sequences after updating ($t(31) = 0.037$, $p = 0.971$). Map A after updating was not more similar to Map B before updating (and vice versa) in the connected sequence condition relative to the same comparison in the unconnected sequence condition, suggesting that the enhanced post-updating similarity we observed (**Figure 3b**) is driven by the incorporation of a novel pattern (not present pre-integration) into both Maps of the connected sequence.

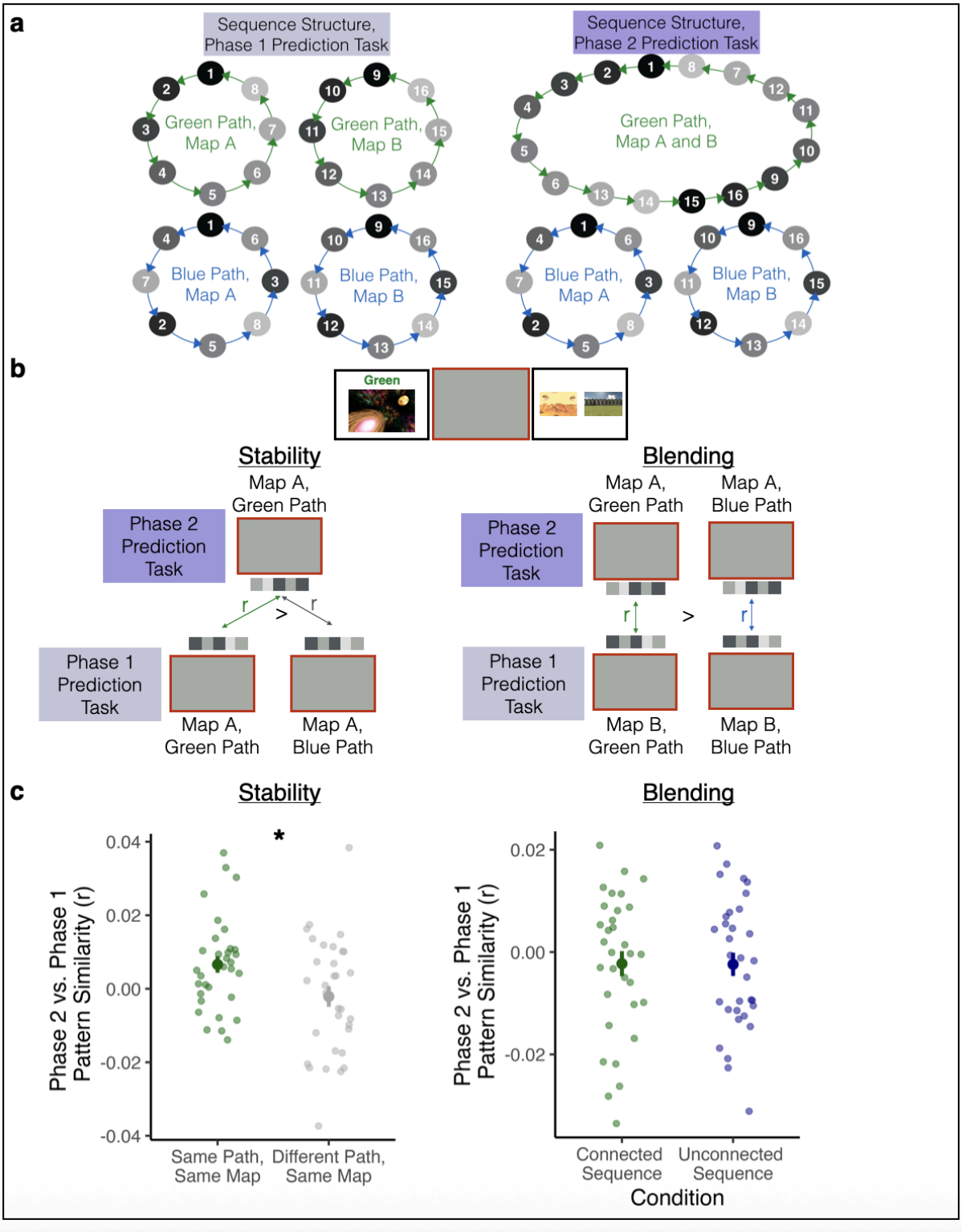

Figure 5 | Stability and Blending of Hippocampal Representations. (a) Sequence structure in the Phase 1 Prediction Task and the Phase 2 Prediction Task. In this example, the green path is the connected sequence and the blue path is the unconnected sequence. **(b)** We analyzed patterns of

brain activity during the blank screen period of the Phase 1 and Phase 2 Prediction Task to investigate both stability and blending of representations in the connected vs. the unconnected sequences. To look for stability in representations, we obtained the correlation between the Phase 2 Prediction Task activity patterns for Map A Green Path trials (connected sequence) and (1) the Phase 1 Prediction Task activity patterns for Map A Green Path trials (same sequence, pre-updating: “same path, same map”) and (2) Phase 1 Prediction Task activity patterns for Map A Blue Path trials (unconnected sequence, “different path, same map”). We completed the same correlations for Map B as well (not shown). Higher correlations between the same path vs. different path would provide evidence of stable representations after integration. To look for evidence of blending, we obtained the correlation between the Phase 2 Prediction Task patterns of activity for Map A Green Path trials (connected sequence) and the Phase 1 Prediction Task patterns of activity for Map B Green Path trials (connected sequence), and vice versa. We then conducted the same comparisons for the Blue Path (unconnected sequence). Higher correlations for the connected vs. unconnected sequence would provide evidence for blended representations after integration. **(c)** Left: Phase 2 vs. Phase 1 pattern similarity was higher for the same path vs. different path, indicating stable representations after updating. Right: Across-map Phase 2 vs. Phase 1 pattern similarity was not significantly different for the connected sequence vs. the unconnected sequence, indicating no evidence for blended representations. Large points indicate the group average pattern similarity, error bars indicate standard error of the mean, and small, transparent points indicate each participant’s across-map pattern similarity. * $p < .05$

Discussion

We investigated when and how temporally extended sequences become integrated in the brain to support novel predictions. Participants rapidly learned novel transitions linking two previously separate sequences, allowing them to successfully anticipate upcoming environments on the new connected sequence immediately after learning. They continued to improve over the course of the experiment, suggesting both rapid and gradual updating of sequence representations. Multivoxel fMRI analyses revealed that hippocampus, but not visual cortex, exhibited increased pattern similarity for previously separate sequences that became connected vs. sequences that remained separate. Hippocampal integration emerged in early runs, suggesting rapid updating of sequence structure in the hippocampus. These integrated representations contained activity patterns from the initial sequences as well as new activity patterns not previously present, and predicted participants’ ability to update their predictions in behavior.

Our findings build on research demonstrating that memories for related experiences – typically, pairwise associations – become integrated in the hippocampus (Schlichting & Preston, 2015). These studies show that when one association (AB) shares features with another (AC), the indirectly related experiences (BC) become represented more similarly in the hippocampus, compared to unrelated pairs [12,19–21,25]. Such integration supports generalization and inferences about indirect relationships [45,46]. More broadly, memory integration may help form structured knowledge, creating internal models or "cognitive maps" that generalize across experiences to guide adaptive behavior [16–18], such as making predictions multiple steps into the future [3].

Unlike studies of pairwise associations that become linked, there are relatively few studies exploring hippocampal integration of large-scale, multistep associations. A recent study addressed this gap, demonstrating that the hippocampus constructs global environment representations that link separately learned routes to support flexible navigation [16]. Participants first learned to navigate within three separate routes in a virtual environment. After a one-day delay, they were taught that the routes were linked and then navigated across them to reach goal locations, requiring a global representation of the newly connected environment. Greater across-route hippocampal similarity *before* the environments were linked predicted more efficient navigation *after* they were linked [16]. Our findings extend this work by showing that integrated sequence representations in the hippocampus (1) emerge rapidly following new learning, (2) preserve stability with initial representations while incorporating new activity patterns, and (3) support flexible multistep predictions in newly connected sequences. Thus, hippocampal memory integration rapidly builds structured representations that guide flexible future-oriented behaviors.

We found that integrated hippocampal representations for the connected vs. unconnected sequence emerged in early runs, immediately after new learning. In contrast, there was no significant difference in pattern similarity between sequence conditions in late runs. We did not detect a significant *difference* between early and late runs, and therefore do not overinterpret the absence of integration in late runs; nevertheless, this pattern of results is somewhat puzzling. Behavioral performance on the Phase 2 Prediction Task continued to improve across runs, raising the question: why did across-map pattern similarity emerge immediately, but not increase further with practice? One possibility is that hippocampal integration is especially useful when task demands are high—such as during early runs, when participants must make multistep judgments across newly linked sequences. Bringing representations of the connected sequences closer together may allow the hippocampus to scaffold these difficult multistep judgments. With increased practice, however, participants may rely less on hippocampal integration to support performance, leading to improved behavior without corresponding increases in hippocampal pattern similarity.

In addition to *when* integrated representations emerge, we also investigated the nature of these representations. We found that individual sequences maintained some stability with their initial representations even after they were updated into a newly connected sequence. However, there was no evidence for blending of the newly connected sequences. This suggests that the post-updating increase in pattern similarity for the previously separate sequences likely reflected the addition of new activity patterns that were not present in each sequence previously. This aligns with prior evidence that de novo representations support insight across related experiences [13]. In our experiment, most of each sequence remained unchanged from pre- to

post-updating: the sequences were linked by two local connections, and the remaining connections were stable over time. Because most connections were unchanged, stability of sequence representations from pre- to post-updating may be more adaptive than the creation of entirely new representations. Nevertheless, it remains unclear whether hippocampal integration of the previously separate sequences was restricted to environments adjacent to the linking environments or whether temporally distant environments also developed more similar representations in the hippocampus. Future research could disentangle these possibilities by increasing the number of trials–particularly trials involving the linking environments–to have sufficient statistical power to determine whether integration occurs even for distant environments.

Prior studies have shown important representational and functional differences between hippocampal subfields and between anterior and posterior hippocampus [14,47–50]. These differences extend to how these hippocampal regions represent overlapping events and sequences [12,49,51–57]. Our analyses were across the hippocampus as a whole because we did not have the spatial resolution to examine different hippocampal subfields. We also restricted our analyses to environment-selective voxels in hippocampus, further limiting our ability to examine subfield or long-axis differences. Future studies with high-resolution fMRI can test whether the integration we observed in our study was limited to certain regions of the hippocampus.

What kind of hippocampal learning mechanisms underlie sequence updating? Our prior work demonstrated that the hippocampus represents temporally extended sequences in a graded manner, with weaker representations for further-away environments [3]. These findings are consistent with computational accounts of successor representations, which propose that internal models cache predictions about successive states, with states weighted according to their

distance [2,58,59]. A feature of successor representations, however, is that novel transitions are not easily incorporated, leading to predictions biased toward the original, pre-update sequence [59]. For example, after learning new transitions within a familiar sequence, predictive hippocampal activity continued to reflect the original successor state rather than the updated one [60]. Recent work suggests that successor representations can be modified more readily in some circumstances, particularly via replay – with even minimal on-task replay sufficient to incorporate novel transitions [61]. In our study, replay between runs may have allowed participants to adjust cached representations, integrating the newly learned transitions to support accurate multistep predictions.

An alternative account is that participants engaged a model-based strategy, explicitly representing each successive link between environments [62]. Unlike successor representations, model-based learning readily supports rapid updating because it explicitly stores information about state-to-state transitions. When new transitions are encountered, the transition model can be directly revised, allowing predictions to be recomputed online from the updated structure [59]. We have found evidence consistent with such a link-based strategy that supports multistep predictions particularly after memory consolidation [36]. Hippocampal representations may flexibly shift between cached successor representations and model-based computations depending on task demands. Future work could disentangle these mechanisms by testing how replay, consolidation, and task demands interact to support the balance between successor representations and model-based learning in hippocampal sequence representations.

In summary, we show that new learning rapidly integrates sequence representations in the hippocampus. The extent to which sequences were integrated was related to the behavioral ability to update multistep predictions. Although participants quickly learned the new sequence

structure, their ability to make predictions about upcoming environments across sequences also improved with time, implying both rapid and gradual updating of learned representations. This opens the door for future work investigating how internal models are both rapidly and gradually updated in the brain. Thus, our work sheds light on how and when internal models are represented and updated, and how they are used to guide flexible and adaptive behavior.

CRediT Statement

Hannah Tarder-Stoll: Conceptualization, Data Curation, Investigation, Methodology, Project Administration, Software, Writing—original draft, Writing—review and editing; **Chris Baldassano**: Conceptualization, Methodology, Funding Acquisition, Project Administration, Resources, Supervision, Writing—original draft, Writing—review and editing; **Mariam Aly**: Conceptualization, Methodology, Funding Acquisition, Project Administration, Resources, Supervision, Writing—original draft, Writing—review and editing.

References

1. Schapiro AC, Kustner LV, Turk-Browne NB. 2012 Shaping of Object Representations in the Human Medial Temporal Lobe Based on Temporal Regularities. *Curr. Biol.* **22**, 1622–1627. (doi:10.1016/j.cub.2012.06.056)

2. Stachenfeld KL, Botvinick MM, Gershman SJ. 2017 The hippocampus as a predictive map. *Nat. Neurosci.* **20**, 1643–1653. (doi:10.1038/nn.4650)

3. Tarder-Stoll H, Baldassano C, Aly M. 2024 The brain hierarchically represents the past and future during multistep anticipation. *Nat. Commun.* **15**, 9094. (doi:10.1038/s41467-024-53293-3)

4. Tolman EC, Honzik CH. 1930 Introduction and removal of reward, and maze performance in rats. *Univ. Calif. Publ. Psychol.* **4**, 257–275.

5. Tolman EC. 1948 Cognitive maps in rats and men. *Psychol. Rev.* **55**, 189–208. (doi:10.1037/h0061626)

6. Treichler FR, Van Tilburg D. 1996 Concurrent conditional discrimination tests of transitive inference by macaque monkeys: List linking. *J. Exp. Psychol. Anim. Behav. Process.* **22**, 105–117. (doi:10.1037/0097-7403.22.1.105)

7. Spiers HJ, Gilbert SJ. 2015 Solving the detour problem in navigation: a model of prefrontal and hippocampal interactions. *Front. Hum. Neurosci.* **9**. (doi:10.3389/fnhum.2015.00125)

8. Epstein RA, Patai EZ, Julian JB, Spiers HJ. 2017 The cognitive map in humans: spatial navigation and beyond. *Nat. Neurosci.* **20**, 1504–1513. (doi:10.1038/nn.4656)

9. Brown TI, Carr VA, LaRocque KF, Favila SE, Gordon AM, Bowles B, Bailenson JN, Wagner AD. 2016 Prospective representation of navigational goals in the human hippocampus. *Science* **352**, 1323–1326. (doi:10.1126/science.aaf0784)

10. Shahbaba B, Li L, Agostinelli F, Saraf M, Cooper KW, Haghverdian D, Elias GA, Baldi P, Fortin NJ. 2022 Hippocampal ensembles represent sequential relationships among an extended sequence of nonspatial events. *Nat. Commun.* **13**, 787. (doi:10.1038/s41467-022-28057-6)

11. Schlichting ML, Preston AR. 2015 Memory integration: neural mechanisms and implications for behavior. *Curr. Opin. Behav. Sci.* **1**, 1–8. (doi:10.1016/j.cobeha.2014.07.005)

12. Schlichting ML, Mumford JA, Preston AR. 2015 Learning-related representational changes reveal dissociable integration and separation signatures in the hippocampus and prefrontal cortex. *Nat. Commun.* **6**, 8151. (doi:10.1038/ncomms9151)

13. Milivojevic B, Vicente-Grabovetsky A, Doeller CF. 2015 Insight Reconfigures Hippocampal-Prefrontal Memories. *Curr. Biol.* **25**, 821–830. (doi:10.1016/j.cub.2015.01.033)

14. Brunec IK, Robin J, Olsen RK, Moscovitch M, Barense MD. 2020 Integration and differentiation of hippocampal memory traces. *Neurosci. Biobehav. Rev.* **118**, 196–208. (doi:10.1016/j.neubiorev.2020.07.024)

15. Cohn-Sheehy BI, Delarazan AI, Reagh ZM, Crivelli-Decker JE, Kim K, Barnett AJ, Zacks JM, Ranganath C. 2021 The hippocampus constructs narrative memories across distant events. *Curr. Biol.* **31**, 4935-4945.e7. (doi:10.1016/j.cub.2021.09.013)

16. Fernandez C, Jiang J, Wang S-F, Choi HL, Wagner AD. 2023 Representational integration and differentiation in the human hippocampus following goal-directed navigation. *eLife* **12**, e80281. (doi:10.7554/eLife.80281)

17. Morton NW, Sherrill KR, Preston AR. 2017 Memory integration constructs maps of space, time, and concepts. *Curr. Opin. Behav. Sci.* **17**, 161–168. (doi:10.1016/j.cobeha.2017.08.007)

18. Sherrill KR, Molitor RJ, Karagoz AB, Atyam M, Mack ML, Preston AR. 2023 Generalization of cognitive maps across space and time. *Cereb. Cortex* **33**, 7971–7992. (doi:10.1093/cercor/bhad092)

19. Schlichting ML, Zeithamova D, Preston AR. 2014 CA1 subfield contributions to memory integration and inference. *Hippocampus* **24**, 1248–1260. (doi:10.1002/hipo.22310)

20. Schlichting ML, Preston AR. 2014 Memory reactivation during rest supports upcoming learning of related content. *Proc. Natl. Acad. Sci.* **111**, 15845–15850. (doi:10.1073/pnas.1404396111)

21. Schlichting ML, Preston AR. 2016 Hippocampal–medial prefrontal circuit supports memory updating during learning and post-encoding rest. *Neurobiol. Learn. Mem.* **134**, 91–106. (doi:10.1016/j.nlm.2015.11.005)

22. Richter FR, Chanales AJH, Kuhl BA. 2016 Predicting the integration of overlapping memories by decoding mnemonic processing states during learning. *NeuroImage* **124**, 323–335. (doi:10.1016/j.neuroimage.2015.08.051)

23. Chanales AJH, Dudukovic NM, Richter FR, Kuhl BA. 2019 Interference between overlapping memories is predicted by neural states during learning. *Nat. Commun.* **10**, 5363. (doi:10.1038/s41467-019-13377-x)

24. van Kesteren MTR, Rignanese P, Gianferrara PG, Krabbendam L, Meeter M. 2020 Congruency and reactivation aid memory integration through reinstatement of prior knowledge. *Sci. Rep.* **10**, 4776. (doi:10.1038/s41598-020-61737-1)

25. Molitor RJ, Sherrill KR, Morton NW, Miller AA, Preston AR. 2021 Memory Reactivation during Learning Simultaneously Promotes Dentate Gyrus/CA2,3 Pattern Differentiation and CA1 Memory Integration. *J. Neurosci.* **41**, 726–738. (doi:10.1523/JNEUROSCI.0394-20.2020)

26. Audrain S, McAndrews MP. 2022 Schemas provide a scaffold for neocortical integration of new memories over time. *Nat. Commun.* **13**, 5795. (doi:10.1038/s41467-022-33517-0)

27. Tompary A, Davachi L. 2017 Consolidation Promotes the Emergence of Representational Overlap in the Hippocampus and Medial Prefrontal Cortex. *Neuron* **96**, 228-241.e5. (doi:10.1016/j.neuron.2017.09.005)

28. Lee SW, O'Doherty JP, Shimojo S. 2015 Neural Computations Mediating One-Shot Learning in the Human Brain. *PLOS Biol.* **13**, e1002137. (doi:10.1371/journal.pbio.1002137)

29. Nelli S, Braun L, Dumbalska T, Saxe A, Summerfield C. 2023 Neural knowledge assembly in humans and neural networks. *Neuron* **111**, 1504-1516.e9. (doi:10.1016/j.neuron.2023.02.014)

30. Bliss TVP, Collingridge GL. 1993 A synaptic model of memory: long-term potentiation in the hippocampus. *Nature* **361**, 31–39. (doi:10.1038/361031a0)

31. Moscovitch M. 2008 The hippocampus as a 'stupid,' domain-specific module: Implications for theories of recent and remote memory, and of imagination. *Can. J. Exp. Psychol. Rev. Can. Psychol. Expérimentale* **62**, 62–79. (doi:10.1037/1196-1961.62.1.62)

32. Prince SM, Cushing SD, Yassine TA, Katragadda N, Roberts TC, Singer AC. 2025 New information triggers prospective codes to adapt for flexible navigation. *Nat. Commun.* **16**, 4822. (doi:10.1038/s41467-025-60122-8)

33. Gupta AS, Meer MAA van der, Touretzky DS, Redish AD. 2010 Hippocampal Replay Is Not a Simple Function of Experience. *Neuron* **65**, 695–705. (doi:10.1016/j.neuron.2010.01.034)

34. Ólafsdóttir HF, Barry C, Saleem AB, Hassabis D, Spiers HJ. 2015 Hippocampal place cells construct reward related sequences through unexplored space. *eLife* **4**, e06063. (doi:10.7554/eLife.06063)

35. Liu Y, Dolan RJ, Kurth-Nelson Z, Behrens TEJ. 2019 Human Replay Spontaneously Reorganizes Experience. *Cell* **178**, 640-652.e14. (doi:10.1016/j.cell.2019.06.012)

36. Tarder-Stoll H, Baldassano C, Aly M. 2024 Consolidation Enhances Sequential Multistep Anticipation but Diminishes Access to Perceptual Features. *Psychol. Sci.* **35**, 1178–1199. (doi:10.1177/09567976241256617)

37. Foster DJ. 2017 Replay Comes of Age. *Annu. Rev. Neurosci.* **40**, 581–602. (doi:10.1146/annurev-neuro-072116-031538)

38. Ólafsdóttir HF, Bush D, Barry C. 2018 The Role of Hippocampal Replay in Memory and Planning. *Curr. Biol.* **28**, R37–R50. (doi:10.1016/j.cub.2017.10.073)

39. Momennejad I, Otto AR, Daw ND, Norman KA. 2018 Offline replay supports planning in human reinforcement learning. *eLife* **7**, e32548. (doi:10.7554/eLife.32548)

40. Bates D, Mächler M, Bolker B, Walker S. 2015 Fitting Linear Mixed-Effects Models Using lme4. *J. Stat. Softw.* **67**, 1–48. (doi:10.18637/jss.v067.i01)

41. Kriegeskorte N, Mur M, Bandettini PA. 2008 Representational similarity analysis - connecting the branches of systems neuroscience. *Front. Syst. Neurosci.* **2**. (doi:10.3389/neuro.06.004.2008)

42. Wang L, Mruczek REB, Arcaro MJ, Kastner S. 2015 Probabilistic Maps of Visual Topography in Human Cortex. *Cereb. Cortex* **25**, 3911–3931. (doi:10.1093/cercor/bhu277)

43. Tarhan L, Konkle T. 2020 Reliability-based voxel selection. *NeuroImage* **207**, 116350. (doi:10.1016/j.neuroimage.2019.116350)

44. Dimsdale-Zucker HR, Ranganath C. 2018 Chapter 27 - Representational Similarity Analyses: A Practical Guide for Functional MRI Applications. In *Handbook of Behavioral Neuroscience* (ed D Manahan-Vaughan), pp. 509–525. Elsevier. (doi:10.1016/B978-0-12-812028-6.00027-6)

45. Zeithamova D, Dominick AL, Preston AR. 2012 Hippocampal and Ventral Medial Prefrontal Activation during Retrieval-Mediated Learning Supports Novel Inference. *Neuron* **75**, 168–179. (doi:10.1016/j.neuron.2012.05.010)

46. Schlichting ML, Preston AR. 2017 The Hippocampus and Memory Integration: Building Knowledge to Navigate Future Decisions. In *The Hippocampus from Cells to Systems: Structure, Connectivity, and Functional Contributions to Memory and Flexible Cognition* (eds DE Hannula, MC Duff), pp. 405–437. Cham: Springer International Publishing. (doi:10.1007/978-3-319-50406-3_13)

47. Poppenk J, Evensmoen HR, Moscovitch M, Nadel L. 2013 Long-axis specialization of the human hippocampus. *Trends Cogn. Sci.* **17**, 230–240. (doi:10.1016/j.tics.2013.03.005)

48. Schapiro AC, Turk-Browne NB, Botvinick MM, Norman KA. 2017 Complementary learning systems within the hippocampus: A neural network modelling approach to reconciling episodic memory with statistical learning. *Philos. Trans. R. Soc. Lond. B. Biol. Sci.* **372**. (doi:10.1098/rstb.2016.0049)

49. Dimsdale-Zucker HR, Ritchey M, Ekstrom AD, Yonelinas AP, Ranganath C. 2018 CA1 and CA3 differentially support spontaneous retrieval of episodic contexts within human hippocampal subfields. *Nat. Commun.* **9**, 294. (doi:10.1038/s41467-017-02752-1)

50. Duncan KD, Schlichting ML. 2018 Hippocampal representations as a function of time, subregion, and brain state. *Neurobiol. Learn. Mem.* **153**, 40–56. (doi:10.1016/j.nlm.2018.03.006)

51. Hulbert JC, Norman KA. 2015 Neural Differentiation Tracks Improved Recall of Competing Memories Following Interleaved Study and Retrieval Practice. *Cereb. Cortex* **25**, 3994–4008. (doi:10.1093/cercor/bhu284)

52. Favila SE, Chanales AJH, Kuhl BA. 2016 Experience-dependent hippocampal pattern differentiation prevents interference during subsequent learning. *Nat. Commun.* **7**, 11066. (doi:10.1038/ncomms11066)

53. Kim G, Norman KA, Turk-Browne NB. 2017 Neural Differentiation of Incorrectly Predicted Memories. *J. Neurosci.* **37**, 2022–2031. (doi:10.1523/JNEUROSCI.3272-16.2017)

54. Hsieh L-T, Gruber MJ, Jenkins LJ, Ranganath C. 2014 Hippocampal Activity Patterns Carry Information about Objects in Temporal Context. *Neuron* **81**, 1165–1178. (doi:10.1016/j.neuron.2014.01.015)

55. Brown TI, Ross RS, Keller JB, Hasselmo ME, Stern CE. 2010 Which Way Was I Going? Contextual Retrieval Supports the Disambiguation of Well Learned Overlapping Navigational Routes. *J. Neurosci.* **30**, 7414–7422. (doi:10.1523/JNEUROSCI.6021-09.2010)

56. Chanales AJH, Oza A, Favila SE, Kuhl BA. 2017 Overlap among Spatial Memories Triggers Repulsion of Hippocampal Representations. *Curr. Biol.* **27**, 2307-2317.e5. (doi:10.1016/j.cub.2017.06.057)

57. Bein O, Davachi L. 2024 Event Integration and Temporal Differentiation: How Hierarchical Knowledge Emerges in Hippocampal Subfields through Learning. *J. Neurosci.* **44**. (doi:10.1523/JNEUROSCI.0627-23.2023)

58. Dayan P. 1993 Improving Generalization for Temporal Difference Learning: The Successor Representation. *Neural Comput.* **5**, 613–624. (doi:10.1162/neco.1993.5.4.613)

59. Momennejad I, Russek EM, Cheong JH, Botvinick MM, Daw ND, Gershman SJ. 2017 The successor representation in human reinforcement learning. *Nat. Hum. Behav.* **1**, 680–692. (doi:10.1038/s41562-017-0180-8)

60. Russek EM, Momennejad I, Botvinick MM, Gershman SJ, Daw ND. 2021 Neural evidence for the successor representation in choice evaluation. , 2021.08.29.458114. (doi:10.1101/2021.08.29.458114)

61. Son J-Y, Vives M-L, Bhandari A, FeldmanHall O. 2024 Replay shapes abstract cognitive maps for efficient social navigation. *Nat. Hum. Behav.* **8**, 2156–2167. (doi:10.1038/s41562-024-01990-w)

62. Daw ND, Dayan P. 2014 The algorithmic anatomy of model-based evaluation. *Philos. Trans. R. Soc. B Biol. Sci.* **369**, 20130478. (doi:10.1098/rstb.2013.0478)